

Tetrahedral-Atom Zincophosphate Structures. Zinc Diethyl Phosphate, $[\text{Zn}(\text{O}_2\text{P}(\text{OC}_2\text{H}_5)_2)_2]_n$, a One-Dimensional Inorganic "Polymer"

William T. A. Harrison,*† Tina M. Nenoff, Thurman E. Gier, and Galen D. Stucky*

Department of Chemistry, University of California, Santa Barbara, California 93106-9510

Received March 3, 1992

The synthesis, structure, and some properties of a new, anhydrous, zinc ethyl phosphate are described. $\text{Zn}(\text{O}_2\text{P}(\text{OC}_2\text{H}_5)_2)_2$ (ZnPOEt) crystallizes in the monoclinic space group $C2/c$ (No. 15) with $a = 22.176$ (6) Å, $b = 8.042$ (2) Å, $c = 9.088$ (3) Å, $\beta = 96.553$ (8)°, $V = 1610$ Å³, $\rho_{\text{calc}} = 1.533$ g/cm³, $\mu = 17.8$ cm⁻¹, and $Z = 4$, with $R(F_o) = 6.94\%$ for 658 observed reflections ($I > 3\sigma(I)$). The novel structure consists of infinite 1-dimensional chains of vertex-linked zinc-oxygen and phosphorus-oxygen tetrahedra forming "four-rings": two of the phosphate P-O vertices are coordinated to ethyl ($-\text{C}_2\text{H}_5$) groups, and the "herringbone" crystal packing is determined by van der Waals' forces between these terminal organic groups. Physical (TGA, DSC) and spectroscopic data (IR, ¹H, and ³¹P NMR) are presented. The physical data show a melting, followed by a decomposition reaction, eventually resulting in $\text{Zn}(\text{PO}_3)_2$. ZnPOEt is soluble in, and recrystallizable from, several polar and nonpolar solvents: the NMR data suggest that ZnPOEt maintains a "polymeric" state in solution. ZnPOEt is contrasted with its sulfur-containing analogue, $\text{Zn}(\text{S}_2\text{P}(\text{OC}_2\text{H}_5)_2)_2$.

Introduction

Over the past few years there has been considerable interest in the structures and properties of layered metal/phosphorus/oxygen/organic phases, composed of organophosphate ($\text{O}_{3-n}\text{P}(\text{OR})_n$, $n = 1, 2$) or organophosphonate (O_3PR) groups, in combination with di- or trivalent metal ions. Several metal-organophosphonate phases, exemplified by the typical formula $\text{M}(\text{O}_3\text{PR}) \cdot \text{H}_2\text{O}$ ($\text{M} = \text{Mg}, \text{Ca}, \text{Mn}, \text{Fe}, \text{Co}, \text{Ni}, \text{Cu}, \text{Zn}, \text{Cd}, \text{etc.}$; $\text{R} = \text{methyl}, \text{ethyl}, \text{phenyl}, \text{etc.}$) were first prepared by Cunningham et al.¹ and structurally studied by Alberti et al.² Mallouk and co-workers prepared a number of divalent metal organophosphonates as single crystals and determined the structure of manganese phenylphosphonate hydrate, $\text{Mn}(\text{O}_3\text{PC}_6\text{H}_5) \cdot \text{H}_2\text{O}$.³ Clearfield and co-workers solved the structures of zinc phenylphosphonate hydrate, $\text{Zn}(\text{O}_3\text{PC}_6\text{H}_5) \cdot \text{H}_2\text{O}$,⁴ and zinc ethyl phosphate hydrate, $\text{Zn}(\text{O}_3\text{POC}_2\text{H}_5) \cdot \text{H}_2\text{O}$, and a functionalized, amide-containing congener, $\text{Zn}(\text{O}_3\text{POC}_2\text{H}_4\text{NH}_2)(\text{O}_2\text{CCH}_3)$, by X-ray diffraction methods.⁵ The layered structure of $\text{VO}(\text{O}_3\text{H}_5\text{PO}_3) \cdot \text{H}_2\text{O}$ has been determined by Huan et al.,⁶ and a new family of ferric phosphonates has been reported,⁷ which contain layers of FeO_6 octahedra and $\text{O}_3\text{PC}_6\text{H}_5$ tetrahedra.

Crystal-structure studies have demonstrated that the above materials contain 2-dimensional layers of M- and P-centered polyhedra, separated by organic groups. These phases have been considered to be model compounds for the industrially-important pillared clays,⁸ since these structures have a well-defined and predictable layer topology. Substitution in the metal coordination

sphere and intercalation reactions have been demonstrated for several of these layered phases.^{8,9}

In this paper we report the synthesis, structure, and some properties of zinc diethyl phosphate, $\text{Zn}(\text{O}_2\text{P}(\text{OC}_2\text{H}_5)_2)_2$ (ZnPOEt), a new zinc organophosphate which has a 1-dimensional chainlike rather than a layered structure: these chains have tetrahedral ionic cores surrounded by hydrocarbon coatings. ZnPOEt is compared to zinc *O,O*-diethyl dithiophosphate, $\text{Zn}(\text{S}_2\text{P}(\text{OC}_2\text{H}_5)_2)_2$ (ZnSEt),^{10,11} a material which has found extensive applicability in lubrication science.¹² However, ZnSEt has a chain connectivity and reactivity different from those of the material reported here.

Experimental Section

Synthesis. The ZnPOEt was prepared hydrothermally: 1.63 g of ZnO, 29.14 g of triethyl phosphate, $(\text{EtO})_3\text{PO}$, and 20 cm³ of water were placed in a Teflon bottle, resulting in a white slurry, which was placed in a 100 °C water bath, enclosed in a well-ventilated fume hood. Ethanol was given off (detected by its odor) and large translucent crystals formed over several days, after which the solution was cooled, and upon washing with methanol, a very large mass of fibrous, intergrown crystals was recovered. The yield was 5.07 g (68% based on ZnO). ZnPOEt appears to be indefinitely stable in air.

Structure Determination. ZnPOEt crystals are extremely soft and easily damaged, but a good-quality, sharply diffracting (typical ω -scan width = 0.17°), needle-shaped translucent crystal (dimensions ca. 0.5 × 0.1 × 0.1 mm) was finally selected and mounted on a thin glass fiber with cyanoacrylate glue. Room-temperature (25 (1)°C) intensity data were collected on a Huber automated four-circle diffractometer (graphite-monochromated $\text{MoK}\alpha$ radiation, $\lambda = 0.71073$ Å), as outlined in Table I. A total of 21 reflections were located and centered by searching reciprocal space and indexed to obtain a unit cell and orientation matrix. The lattice constants were optimized by least-squares refinement, resulting in the following monoclinic parameters: $a = 22.176$ (6) Å, $b = 8.042$ (2) Å, $c = 9.088$ (3) Å, $\beta = 96.553$ (8)°, $V = 1610$ Å³. A total of 2358 unique intensity data were collected using the θ - 2θ scanning mode between 0 and 45° in 2θ , with standard reflections monitored for intensity variation throughout the course of the experiment: no significant variation in standards was observed. The scan speed was 3°/min with a scan range of 1.4° below $\text{K}\alpha_1$ to 1.5° above $\text{K}\alpha_2$. Crystal absorption was monitored

* Authors for correspondence.

† Department of Chemistry, University of Houston, Houston, TX 77204-5641.

- (1) Cunningham, D.; Hennely, P. J. D.; Deeney, T. *Inorg. Chim. Acta* **1979**, *37*, 95.
- (2) Alberti, G.; Costantino, U.; Alluli, S.; Tomassini, J. *J. Inorg. Nucl. Chem.* **1978**, *40*, 1113.
- (3) Cao, G.; Lee, H.; Lynch, V. M.; Mallouk, T. E. *Inorg. Chem.* **1988**, *27*, 2781.
- (4) Martin, K.; Squattrito, P. J.; Clearfield, A. *Inorg. Chim. Acta* **1989**, *155*, 7.
- (5) Ortiz-Avila, Y.; Rudolph, P. R.; Clearfield, A. *Inorg. Chem.* **1989**, *28*, 2137.
- (6) Huan, G.; Jacobsen, A. J.; Johnson, J. W.; Corcoran, E. W., Jr. *Chem. Mater.* **1990**, *2*, 91.
- (7) Bujoli, B.; Palvadeau, P.; Rouxel, J. *Chem. Mater.* **1990**, *2*, 582.
- (8) Frink, K. J.; Wang, R.-C.; Colón, J. L.; Clearfield, A. *Inorg. Chem.* **1991**, *30*, 1438.

(9) Cao, G.; Mallouk, T. E. *Inorg. Chem.* **1991**, *30*, 1434.

(10) Ito, T.; Igarashi, T.; Hagihara, H. *Acta Crystallogr.* **1969**, *B25*, 2303.

(11) Burn, A. J.; Dewan, S. K.; Gosney, I.; Tan, P. S. G. *J. Chem. Soc., Perkin Trans.* **1990**, 753.

(12) Ford, J. F. *J. Inst. Pet.* **1968**, *54*, 200.

Table I. Crystallographic Parameters for $\text{Zn}(\text{O}_2\text{P}(\text{OC}_2\text{H}_5)_2)_2$

empirical formula	$\text{ZnP}_2\text{O}_8\text{C}_8\text{H}_{20}$	Z	4
fw	371.4	T ($^\circ\text{C}$)	25 (1)
space group	$C2/c$ (No. 15)	λ (Mo $K\alpha$) (\AA)	0.710 73
a (\AA)	22.176 (6)	ρ_{calc} (g/cm^3)	1.533
b (\AA)	8.042 (2)	μ (Mo $K\alpha$) (cm^{-1})	17.8
c (\AA)	9.088 (3)	$R(F_o)^a$ (%)	6.94
β (deg)	96.553 (8)	$R_w(F_o)^b$ (%)	6.21
V (\AA^3)	1610		

$$^a R = \sum |F_o| - |F_c| / \sum |F_o|. \quad ^b R_w = [\sum w(|F_o| - |F_c|)^2 / \sum w|F_o|^2]^{1/2}.$$

by using ψ -scans through 360° for selected reflections with $\chi \approx 90^\circ$. Absorption was negligible, and no correction was applied to the data. The raw data were reduced using a Lehmann-Larsen profile-fitting routine,¹³ and the normal corrections for Lorentz and polarization effects were made. All the data collection and reduction routines were based on the UCLA package.¹⁴ After data merging to 678 unique intensities (observability criterion $I > 3\sigma(I)$; $R_M = 2.4\%$), systematic absences (hkl , $h+k$; $h0l$, h, l ; $0k0$, k) were compatible with space groups Cc and $C2/c$. The number of observed reflections, expressed as a percentage of the total number possible in the molybdenum sphere, was only 28%. However, this is compatible to the 31% of reflections found to have measurable intensities in the structure determination of $\text{Zn}(\text{S}_2\text{P}(\text{OC}_2\text{H}_5)_2)_2$.¹⁰

The structure was solved by direct methods, assuming the space group was centrosymmetric $C2/c$ (No. 15), as confirmed by the course of the subsequent refinement. A chemically-reasonable direct-methods solution for all the non-hydrogen atoms was obtained from the program SHELXS-86.¹⁵ No reasonable proton locations could be determined from difference Fourier syntheses, and after anisotropic refinement, all the proton positions were located geometrically on their respective carbon atoms. The protons were attached to the carbon atoms assuming sp^3 geometry around these species: for the three terminal protons attached to C(2) and C(4) the torsion angle $\varphi(\text{O}-\text{C}-\text{H})$ for one of the three methyl hydrogen atoms was set at 180° . The protons were then refined by riding on their respective carbon atoms with the distance and angle constraints of $d(\text{C}-\text{H}) = 0.95 \text{ \AA}$ and $\xi(\text{H}-\text{C}-\text{H}) = 109^\circ$, respectively. Final agreement factors of $R(F) = 6.94\%$ and $R_w(F) = 6.21\%$ ($w_i = 1$) were obtained, as defined in Table I. The least-squares and subsidiary calculations were performed by using the Oxford CRYSTALS system,¹⁶ running on a DEC $\mu\text{VAX-II}$ computer. Final full-matrix refinements were against F and included anisotropic temperature factors (hydrogen thermal parameters were not refined) and a secondary extinction correction¹⁷ (refined value = 121 (11)). Neutral-atom scattering factors were obtained from ref 18. Final Fourier difference maps revealed no regions of significant electron density (minimum = $-0.4 \text{ e}/\text{\AA}^3$, maximum = $0.5 \text{ e}/\text{\AA}^3$). Tables of observed and calculated structure factors are available from the authors.

X-ray powder data (Scintag automated PAD-X diffractometer, θ - θ geometry, flat plate sample, Cu $K\alpha$ radiation, $\lambda = 1.541 78 \text{ \AA}$, $T = 25$ (2) $^\circ\text{C}$) were collected for a crushed sample of ZnPOEt. The instrumental $K\alpha_1/K\alpha_2$ profile was reduced to a single Cu $K\alpha_1$ peak ($\lambda = 1.540 568 \text{ \AA}$) by a stripping routine, and d spacings were established using silicon powder ($a = 5.430 35 \text{ \AA}$) as an internal standard, relative to this wavelength. The data were of insufficient resolution to reveal any observable $K\alpha_1/K\alpha_2$ splitting. The pattern could be indexed with monoclinic cell parameters determined in the single-crystal study, and the powder lattice parameters were optimized by least-squares refinements using Scintag software routines, resulting in the refined values listed in Table II. The pattern was successfully simulated in terms of line positions and intensities with LAZY-PULVERIX¹⁹ using the single-crystal structural parameters described below. Many calculated positions were too weak to be observed, but no evidence for other phases was visible from inspection of the powder data.

Table II. X-ray Powder Data for $\text{Zn}(\text{O}_2\text{P}(\text{OC}_2\text{H}_5)_2)_2$ [Monoclinic, $a = 22.193$ (13) \AA , $b = 8.041$ (4), $c = 9.091$ (8) \AA , $\beta = 96.44$ (4) $^\circ$]

h	k	l	$2\theta_{\text{obs}}$	$\Delta 2\theta^a$	d_{calc}	$I(\text{rel})$
2	0	0	8.050	0.010	11.027	100
1	1	0	11.730	-0.003	7.554	72
1	1	-1	15.000	-0.012	5.908	1
1	1	1	15.602	0.009	5.689	4
3	1	0	16.365	0.012	5.425	6
3	1	-1	18.364	-0.014	4.831	6
3	1	1	19.790	0.005	4.490	2
2	0	2	22.111	0.013	4.024	2
5	1	0	23.022	0.015	3.867	16
1	1	2	23.355	0.015	3.813	3
4	0	-2	24.037	-0.001	3.703	3
6	0	0	24.219	-0.003	3.676	2
3	1	-2	24.578	-0.010	3.622	0 ^b
2	2	-1	25.183	-0.028	3.533	3
2	2	1	25.934	0.013	3.438	1
4	0	2	26.925	0.035	3.316	1
3	1	2	26.730	0.018	3.338	0 ^b
4	2	0	27.458	-0.003	3.248	3
6	0	-2	29.545	-0.023	3.021	1
0	2	2	29.718	-0.036	3.003	1
4	2	-1	28.563	-0.022	3.123	0 ^b
2	2	-2	30.264	0.004	2.954	0 ^b
7	1	0	30.479	0.002	2.933	0 ^b
2	2	2	31.448	-0.006	2.844	0 ^b
5	1	2	31.837	-0.075	2.804	0 ^b
6	2	0	33.037	0.016	2.713	3
8	0	-2	36.283	0.063	2.480	0 ^b
5	3	0	39.340	0.010	2.291	0 ^b
8	2	0	39.637	0.001	2.274	0 ^b
7	3	0	44.357	-0.006	2.041	1
4	4	0	48.150	-0.019	1.889	1
11	1	-2	48.885	-0.025	1.862	0 ^b
0	4	2	49.672	0.047	1.837	0 ^b

$$^a 2\theta_{\text{obs}} - 2\theta_{\text{calc}}. \quad ^b I < I_{\text{max}}/100.$$

Intercalation Studies. The novel structure of ZnPOEt (vide infra) and previous studies on similar compounds^{7,8} suggested that intercalation of other species in the structure might be possible. No inclusion was observed, but ZnPOEt is soluble to various degrees in several polar and nonpolar organic solvents, including methanol, ethanol, cyclohexane, and substituted xylenes.

ZnPOEt was redissolved in hot water, then ethanol was added, and the mixture was cooled. Giant needlelike crystals (typical dimensions $20 \times 0.5 \times 0.5 \text{ mm}$) readily crystallized. The powder pattern of the ground, recrystallized product is identical to that of the starting material, ZnPOEt. The powdered starting material is sparingly soluble in cyclohexane at room temperature, resulting in a translucent solution. Upon evaporation, poor-quality crystals of the starting phase of ZnPOEt were recovered. ZnPOEt was also dissolved in hot xylene, resulting in a perfectly clear solution, which was filtered through $0.2\text{-}\mu\text{m}$ filter paper to ensure the absence of gross nucleating sites: no residue was recovered. Cooling the solution yielded crystals of the original material with no evidence for xylene incorporation.

Physical and Spectroscopic Studies. Differential scanning calorimetry was carried out on ground crystals of ZnPOEt using a DuPont 2000 scanning calorimeter, with a heating rate of $10^\circ\text{C}/\text{min}$. TGA data were collected on a DuPont 9900 thermogravimetric analysis machine in air, using a heating rate of $10^\circ\text{C}/\text{min}$. The infrared spectrum of a disk of finely ground ZnPOEt/KBr was recorded on a BioRad FTS-60 diffuse reflectance spectrometer as described previously.¹ ^1H NMR data were collected on a Nicolet NT300 spectrometer. A 0.1-g sample of ZnPOEt was dissolved in deuterated methanol, and data were collected at 300.5 MHz (field strength 7.05 T) with 24 acquisitions. ^{31}P liquid-state NMR data were obtained using a General Electric GN-300 spectrometer system at 121.65 MHz (field strength 7.05 T) with 2122 acquisitions. ^{31}P peak positions were established relative to standard 85% H_3PO_4 .

Results

Crystal Structure. The asymmetric unit of ZnPOEt is shown in Figure 1, with the complete unit-cell contents illustrated in Figure 2. Final atomic positional and isotropic thermal parameters are listed in Table III, with selected bond distance/angle

(13) Lehmann, M. S.; Larsen, F. K. *Acta Crystallogr.* 1974, *A30*, 580.

(14) Data collection and reduction were controlled using a locally modified version of the UCLA Crystallographic Computing Package, developed by C. E. Strouse, Department of Chemistry, UCLA, Los Angeles, CA.

(15) Sheldrick, G. M. *SHELXS-86 User Guide*; Crystallography Department, University of Göttingen: Göttingen, Germany, 1986.

(16) Watkin, D. J.; Carruthers, J. R.; Betteridge, P. W. *CRYSTALS User Guide*; Chemical Crystallography Laboratory, Oxford University: Oxford, U.K. 1985.

(17) Larson, A. C. In *Crystallographic Computing*; Ahmed, F. R., Ed.; Munksgaard: Copenhagen, 1970; p 291.

(18) Cromer, D. T. *International Tables for X-Ray Crystallography*; Kynoch Press: Birmingham, U.K., 1974; Volume IV, Table 2.3.1.

(19) Yvon, K.; Jeitscho, W.; Parthe, E. J. *Appl. Crystallogr.* 1977, *10*, 73.

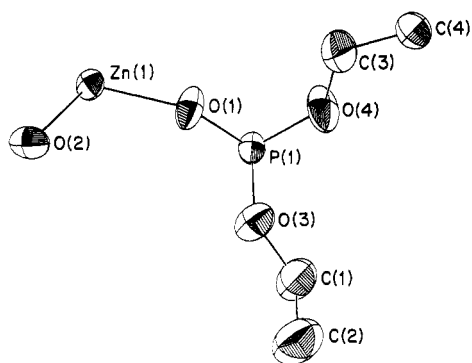


Figure 1. ORTEP²³ view of the asymmetric unit of $\text{Zn}(\text{O}_2\text{P}(\text{OC}_2\text{H}_5)_2)_2$, showing the atom labeling scheme and 20% probability ellipsoids. Protons are omitted for clarity.

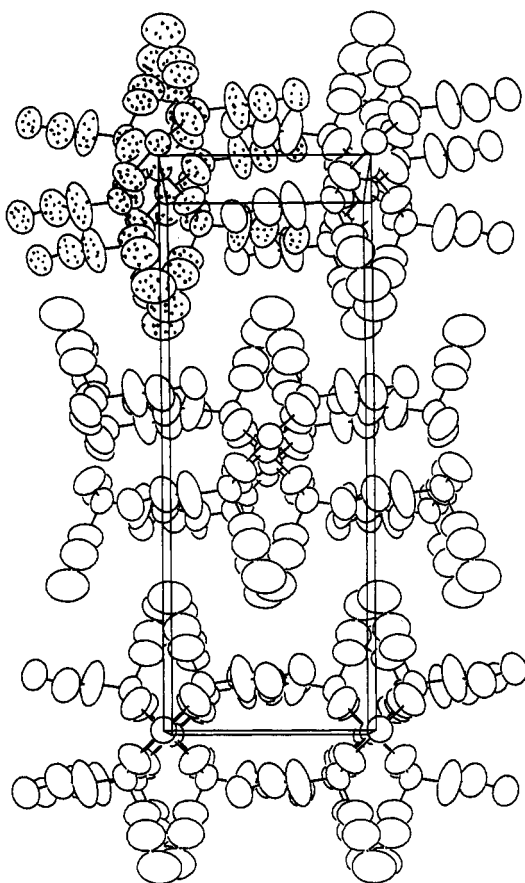


Figure 2. Packing diagram for $\text{Zn}(\text{O}_2\text{P}(\text{OC}_2\text{H}_5)_2)_2$, viewed down the *b*-direction. One chain is indicated by stippling, showing *interchain* herringbone packing in the *c*-direction and *intrachain* packing in the *a*-direction.

data in Table IV. The asymmetric unit of ZnPOEt consists of one zinc atom, one phosphorus atom, four oxygen atoms, four carbon atoms, and ten protons.

The zinc atom is on a 4-fold special position (Wyckoff position: 4e; site symmetry 2) and the other atoms are on general 8-fold crystallographic sites. Both the zinc and phosphorus atoms are tetrahedrally coordinated by oxygen atoms: each zinc atom makes four Zn–O–P bonds, two via O(1) and two via O(2), to two different P atoms. The P atom is surrounded by one each of the crystallographically-distinct oxygen atoms and bonds to two distinct zinc atom neighbors, via O(1) and O(2). The average Zn–O bond length is 1.90 (1) Å, and the average O–Zn–O angle is 109 (1)°. Values for the PO_4 tetrahedron are 1.46 (1) Å (oxygen atoms bonded to P and Zn), 1.55 (2) Å (O's bonded to P and C), and 109 (2)° (O–P–O angle). Due to the large thermal factors

Table III. Atomic Positional Parameters for $\text{Zn}(\text{O}_2\text{P}(\text{OC}_2\text{H}_5)_2)_2$

atom	x	y	z	U_{eq}^a
Zn(1) ^b	0	−0.0084 (3)	1/4	0.0829
P(1)	0.0804 (2)	−0.1853 (5)	0.5228 (3)	0.0881
O(1)	0.0525 (4)	−0.151 (1)	0.3728 (8)	0.1161
O(2)	0.0490 (4)	0.132 (1)	0.1468 (9)	0.1159
O(3)	0.1454 (5)	−0.106 (1)	0.531 (1)	0.1424
O(4)	0.0915 (7)	−0.372 (1)	0.548 (1)	0.1439
C(1)	0.1814 (8)	−0.084 (3)	0.661 (2)	0.1778
C(2)	0.2364 (9)	−0.025 (3)	0.651 (2)	0.2393
C(3)	0.0867 (9)	−0.494 (2)	0.458 (2)	0.1690
C(4)	0.1066 (7)	−0.649 (2)	0.508 (2)	0.1385

^a U_{eq} (Å²) = $(U_1U_2U_3)^{1/3}$. ^b Wyckoff site 4e.

Table IV. Bond Distances (Å) and Angles (deg) for $\text{Zn}(\text{O}_2\text{P}(\text{OC}_2\text{H}_5)_2)_2$

Zn(1)–O(1)	1.903 (8) × 2	Zn(1)–O(2)	1.888 (8) × 2
P(1)–O(1)	1.458 (8)	P(1)–O(2)	1.456 (8)
P(1)–O(3)	1.57 (1)	P(1)–O(4)	1.53 (1)
O(3)–C(1)	1.36 (2)	O(4)–C(3)	1.27 (2)
C(1)–C(2)	1.32 (2)	C(3)–C(4)	1.39 (2)
O(1)–Zn(1)–O(1)′	105.8 (6)	O(2)–Zn(1)–O(1)	107.6 (4)
O(2)–Zn(1)–O(1)	114.7 (3)	O(2)–Zn(1)–O(2)′	106.7 (6)
O(2)–P(1)–O(1)	118.6 (5)	O(3)–P(1)–O(1)	104.9 (6)
O(3)–P(1)–O(2)	111.1 (6)	O(4)–P(1)–O(1)	111.5 (6)
O(4)–P(1)–O(2)	104.9 (6)	O(4)–P(1)–O(3)	105.1 (8)
P(1)–O(1)–Zn(1)	145.9 (6)	P(1)–O(2)–Zn(1)	156.1 (6)
C(1)–O(3)–P(1)	122.5 (11)	C(3)–O(4)–P(1)	131.2 (12)
C(2)–C(1)–O(3)	115.8 (20)	C(4)–C(3)–O(4)	118.9 (16)

of the chain atoms, a rigid-body-motion analysis²⁰ was carried out for the ZnO_4 and PO_4 groups. The behavior of both moieties could be successfully described by the L component of the TLS analysis, with the T and S components having negligible magnitudes, indicating that libration about the central atom was the dominant group motion for both species. Libration-corrected bond lengths for Zn–O, P–O (to Zn), and P–O (to C) were calculated to be 1.92 (1), 1.50 (1), and 1.62 (1) Å, respectively, whilst the corrected bond angles were virtually unchanged from their as-refined values. This connectivity of Zn, P, and O creates an infinite chain of stoichiometry $\text{ZnP}_2\text{O}_4^{4+}$, which propagates in the *c* unit cell direction. The other two phosphorus vertices (O(3) and O(4)) are part of the ethoxide (–OEt) groups, resulting in a chain (and molecular) stoichiometry of $\text{Zn}(\text{O}_2\text{P}(\text{OEt})_2)_2$, schematically illustrated in Figure 3. By way of contradistinction, the thermal parameter situation in the related $\text{Zn}(\text{S}_2\text{P}(\text{OEt})_2)_2$ ^{10,21} could not be successfully analyzed by a rigid-body vibration formalism.

There are two distinct ethoxy configurations in each chain in ZnPOEt . Adjacent –OEt(1) units, composed of –O(3)–C(1)–C(2) (hydrogens omitted), packed in an interleaved “herringbone” configuration with next-neighbors in the *same* chain. Adjacent –OEt(2) groups (–O(4)–C(3)–C(4)) form a herringbone array with the equivalent group in *adjacent* chains. Thus, there are *no* direct connections or hydrogen bonds between adjacent chains, and van der Waals’ interchain contact in the *a*-direction is via corrugated sheets of –OEt(1) groups and in the *b*-direction is via interleaved, herringbone contacts of –OEt(2) entities. Oxygen–carbon torsion angles (φ) for both ethoxy chains are similar: for P(1)–O(3)–C(1)–C(2), $\varphi = 175 (1)^\circ$ and, for P(1)–O(4)–C(3)–C(4), $\varphi = 173 (1)^\circ$, indicating that both chains are close to their ideal anti configuration, expected on simple steric grounds alone. Close interchain nonbonded C–C contacts include C(1)–C(4) (4.05 (3) Å), C(3)–C(3)′ (4.01 (5) Å), and C(2)–C(3) and C(2)–C(4) (both 4.16 (3) Å), in good agreement with expected van der Waals’ contacts for these methylene and methyl species and similar to the values determined for nonbinding C⋯C contacts in the sulfur-containing analogue, $\text{Zn}(\text{S}_2\text{P}(\text{OEt})_2)_2$.¹⁰

(20) Shoemaker, V.; Trueblood, K. N. *Acta Crystallogr.* **1969**, *B24*, 63.
(21) Cruickshank, D. W. J. *Acta Crystallogr.* **1961**, *14*, 896.

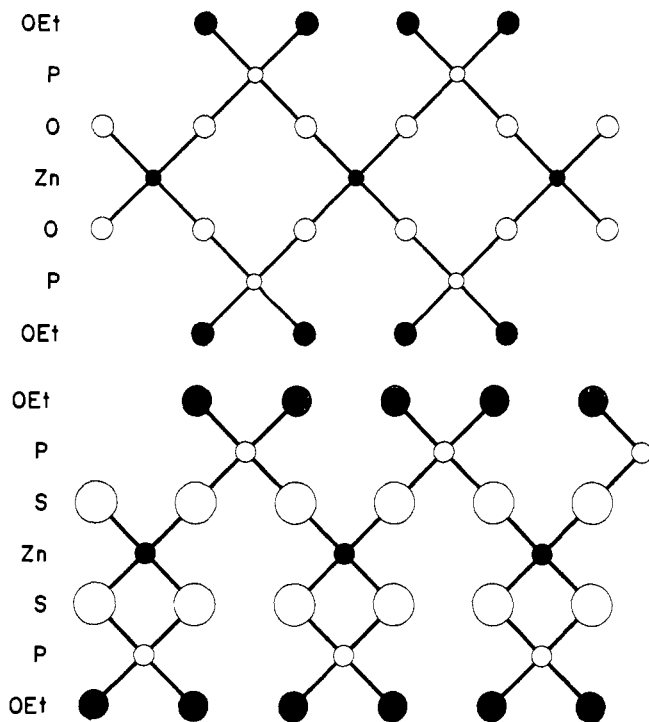


Figure 3. Schematic views of the chain connectivity in (a, top) $\text{Zn}(\text{O}_2\text{P}(\text{OC}_2\text{H}_5)_2)_2$ and (b, bottom) $\text{Zn}(\text{S}_2\text{P}(\text{OC}_2\text{H}_5)_2)_2$, showing the distinct "double" and "single" tetrahedral chains, respectively.

However, the Zn/S/P and chain-chain connectivities in $\text{Zn}(\text{S}_2\text{P}(\text{OEt})_2)_2$ are different from the situation in ZnPOEt (see Figure 3). Topologically, in ZnPOEt , each diethyl phosphate group bridges two adjacent zinc atoms, leading to a chain of (O-atom-bridged) "four-rings" of Zn and P centers, while in ZnPSEt , one *O,O*-diethyl dithiophosphate group bridges adjacent zinc atoms, and the other chelates to the same Zn atom. Hence, in ZnPSEt , a single Zn-S-P-S-Zn "polymeric" strand propagates through the structure, as opposed to the double strand in ZnPOEt . This difference is doubtless partly due to a size effect ($d(\text{Zn}-\text{O}) \sim 1.94 \text{ \AA}$, $d(\text{Zn}-\text{S}) \sim 2.36 \text{ \AA}$), but it is also worthy of note that in ZnPSEt the van der Waals' bonding interactions are more complex, also involving S...C interactions as short as 3.7 \AA .¹⁰

Structure Analysis. A variety of analytical methods have been used to confirm and elaborate upon the $\text{Zn}(\text{O}_2\text{P}(\text{OEt})_2)_2$ repeat unit of this structure, as determined by X-ray crystallography. A TGA analysis of this material reveals the onset of decomposition (loss of diethyl ether) at about $225 \text{ }^\circ\text{C}$, with the reaction being complete at $325 \text{ }^\circ\text{C}$. The residue, heated to $800 \text{ }^\circ\text{C}$, showed a clean X-ray diffraction pattern of $\text{Zn}(\text{PO}_3)_2$. The weakness of the van der Waals' bonds between chains is indicated by the softness of the crystals and the fact that a DSC analysis did not show a heat effect at the melting point, but only the endothermic decomposition at about $300 \text{ }^\circ\text{C}$. Carefully dried ZnPOEt melts at $168\text{--}175 \text{ }^\circ\text{C}$ to a syrup which recrystallizes to a product identical to the original material (comparison of X-ray powder patterns (if the cooling is carried out slowly enough). However, holding the ZnPOEt syrup at $200 \text{ }^\circ\text{C}$ for 2 days suffices to vaporize all of the organic moiety, leaving a dark-colored amorphous residue.

As noted above, ZnPOEt is soluble in water, methanol, and xylenes. The length of the oligomeric unit (in aqueous solution) has been studied through the use of ^1H and ^{31}P NMR. Disregarding solvent peaks, the characteristic methylene and methyl peaks of the $-\text{OEt}$ side chains of ZnPOEt are evident (Figure 4a): a quintuplet, centered at 2.729 ppm , is attributable to the methylene group; these two protons are split into a quadruplet by the methyl protons. It is then further split by the phosphorus into a doublet. For the methyl group (Figure 4b), a distinct triplet centered at 0.690 ppm is shadowed by a much

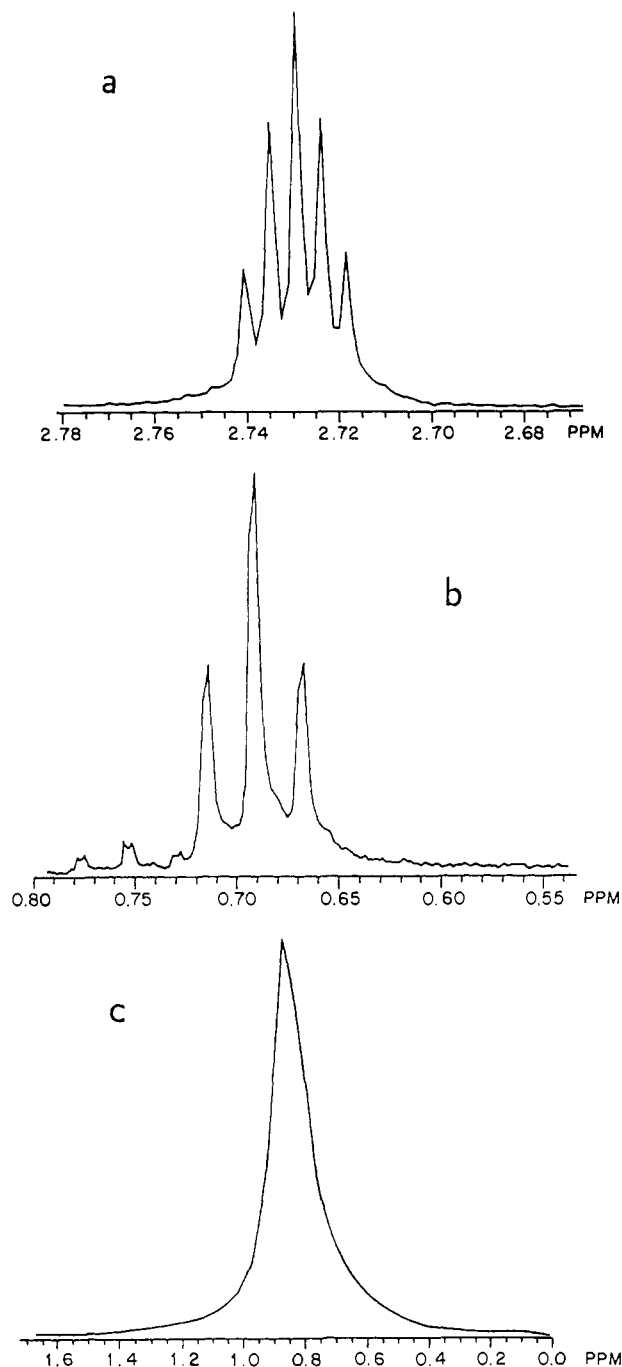


Figure 4. NMR spectra for $\text{Zn}(\text{O}_2\text{P}(\text{OC}_2\text{H}_5)_2)_2$: (a) methylene ($-\text{CH}_2-$) protons; (b) methyl ($-\text{CH}_3$) protons; (c) phosphorus atoms.

smaller triplet centered at 0.755 ppm ($^3J_{\text{H}} 7.2 \text{ Hz}$, $^3J_{\text{PH}} 1.27 \text{ Hz}$). A peak integration shows that the larger set is in a 5:1 ratio with the smaller set.

One explanation for the "double" methyl signal is that the solution-phase zinc organophosphonate is made up of a distinct number of repeating $\text{Zn}(\text{O}_2\text{P}(\text{OEt})_2)_2$ units. The end units' protons will be different than the inner units' protons, as seen by the observed shift and by the small doublet splits due to phosphorus coupling. An approximate chain length has been determined by integration to contain two end and ten inner units, for a total of twelve zinc diethyl phosphate units in a chain, i.e., $[\text{Zn}(\text{O}_2\text{P}(\text{OEt})_2)_2]_{12}$. Conversely, for $\text{Zn}(\text{S}_2\text{P}(\text{OEt})_2)_2$, a monomeric solution species was indicated.¹⁰

The ^{31}P NMR spectrum of ZnPOEt (Figure 4c) shows a singlet at 0.849 ppm , with a slight shoulder at approximately 0.820 ppm . This too can be explained as two different phosphorus atoms, one greatly outnumbering the other due to unit location on the chain.

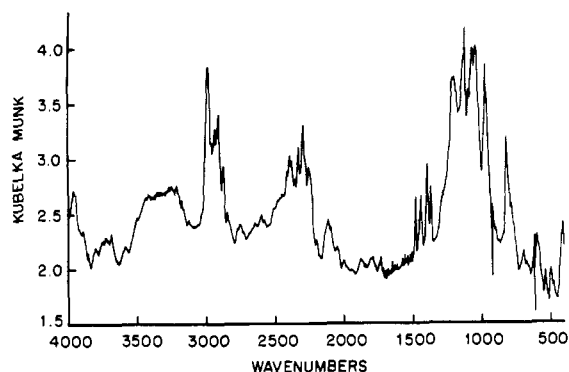


Figure 5. Infrared spectrum of $\text{Zn}(\text{O}_2\text{P}(\text{OC}_2\text{H}_5)_2)_2$.

The diffuse-reflectance infrared spectrum of ZnPOEt is illustrated in Figure 5. The methane and methylene C–H stretches are evident from 2800 to 3000 cm^{-1} , the P–O–C (aliphatic) stretches in the 2200–2500- cm^{-1} and the 1500- cm^{-1} regions, and the Zn/P/O “framework” in the region 1000–500 cm^{-1} . These latter bands are qualitatively similar to those observed for other metal–organophosphonate/phosphate phases,⁸ while the characteristic, strong O–H stretch bands seen in materials which contain a metal-coordinated water² ($\nu \approx 3300\text{--}3500 \text{ cm}^{-1}$) are absent in this structure. We attribute the weak –OH broad-band stretch to be from water in the KBr used for dilution of the sample.

Discussion

$\text{Zn}(\text{PO}_2(\text{OC}_2\text{H}_5)_2)_2$ (ZnPOEt) represents yet another type of zinc organophosphate, distinctly different from previously known species. In $\text{Zn}(\text{O}_3\text{PC}_6\text{H}_5)_2 \cdot \text{H}_2\text{O}$, the zinc atom is octahedrally coordinated by phosphonate-group oxygen atoms and water molecules, resulting in a layerlike “ionic” structure, with the phenyl groups separating adjacent sheets. A similar structure was also found for $\text{Mn}(\text{O}_3\text{PC}_6\text{H}_5)_2 \cdot \text{H}_2\text{O}$. In $\text{Zn}(\text{O}_3\text{POC}_2\text{H}_5)_2 \cdot \text{H}_2\text{O}$ (ZnPOEtW) and $\text{Zn}(\text{O}_3\text{POC}_2\text{H}_4\text{NH}_3)(\text{O}_2\text{CCH}_3)$ (ZnPOEtN), the zinc atom is tetrahedral, with one vertex occupied by a water molecule in ZnPOEtW and one vertex by an acetate ion in ZnPOEtN. These species are also layered, and H bonding plays an important role in establishing the structure, as well as van der Waals’ interlayer bonding. The mobility of the coordinated water in the $\text{M}(\text{O}_3\text{PR})_2 \cdot \text{H}_2\text{O}$ structures has already been demonstrated.^{1,7,8}

In ZnPOEt, as in ZnPSEt, chains, rather than layers, are the structural motif, which here may be considered to have “ionic” Zn/P/O cores and “covalent” C/H exterior surfaces. The tetrahedral zinc atom only sees oxygen atoms, all of which are bound to ethyl phosphate groups as Zn–O–P links, with typical bond distance/angle parameters. There are no layer-building H bonds in ZnPOEt, and adjacent chains are only loosely bonded through van der Waals’ forces. The combination of the ionic core and hydrophobic exterior of these chains allows ZnPOEt to dissolve in several polar and nonpolar solvents, but no inclusion chemistry has yet been shown to occur. Spectral data suggest an average length of about 12 repeating units of the ZnPOEt chain in methanol solution.

ZnPOEt shows certain characteristics of a polymer, viz. the infinite hydrophobic chains, interacting through van der Waals’ forces. However, in ZnPOEt these chains are highly aligned, presumably by bonding requirements of the zinc/phosphate 1-dimensional core, to the extent of forming a normal, sharply diffracting crystal, although the large thermal factors of the terminal ethyl groups (vide supra) indicate a considerable degree of static/dynamic disorder in these groups. Questions such as the relative importance of ionic bonding in the chain cores and covalent interactions of the hydrocarbon chain exteriors and if the chains may make collective motion relative to each other need to be resolved. ZnPOEt may even serve as a model compound for highly-aligned polymers,²² and further experiments are now in progress to examine these effects in ZnPOEt and related materials. ZnPSEt has been used extensively as an antiwear and antioxidant in lubricants.¹² Whether ZnPOEt has any technological applications as an oil additive also merits further investigation—for instance, the above experiments indicate that it (ZnPOEt) appears to be more resilient to degradation by hydrolysis than its sulfur-containing analogue.¹¹

Acknowledgment. We thank Nancy Keder for crystallographic assistance, R. S. “Bob” Maxwell for assistance in recording the spectroscopic data, and the National Science Foundation (Grant DMR920B511) and Office of Naval Research for partial funding.

Supplementary Material Available: Tables of anisotropic thermal factors and hydrogen atom coordinates (2 pages). Ordering information is given on any current masthead page.

- (22) Samuels, R. J. *Structured Polymer Properties: the Identification, Interpretation, and Application of Crystalline Polymer Structure*; Wiley: New York, 1974.
- (23) Johnson, C. K. Oak Ridge National Laboratory Report ORNL-5138; Oak Ridge, TN 37830, 1976 (with local modifications).